Asian Journal of Chemistry; Vol. 33, No. 5 (2021), 1031-1038

ASIAN JOURNAL OF CHEMISTRY

https://doi.org/10.14233/ajchem.2021.23100

COVID-19 Protease Inhibitor using Azole *N*-Mannich Bases: A Molecular Docking Approach

K.N. ARATHI[1,*], K. ABDUL KHAYUM[2], SULAIMAN MOHAMMED ALNASSER[3] and ONSINYO JAMES MEROKA[4]

[1]Department of Pharmaceutical Chemistry, Sanjo College of Pharmaceutical Studies, Palakkad-678702, India
[2]Department of Pharmacology, PSG College of Pharmacy, Coimbatore-641004, India
[3]Department of Pharmacology and Toxicology, Unaizah College of Pharmacy, Qassim University, Saudi Arabia
[4]Department of Pharmacology, Mount Kenya University, Thika, Kenya

*Corresponding author: E-mail: kn.arathi@gmail.com

Received: 18 December 2020; *Accepted*: 23 February 2021; *Published online*: 16 April 2021; AJC-20322

Coronaviruses are the largest group of viruses belonging to the *Nidovirales* order, which includes *Coronaviridae*, *Arteriviridae* and *Roniviridae* families. In this work, a molecular modeling technique is adopted to find out the excellent moiety to inhibit the protease enzyme which is present in the coronavirus. Autodock 4.2 tool was used to find out the docking score of 32 ligands. The molinspiration server helps to find out the drug-likeness property and whether these ligands having a binding towards the protease enzyme. The synthetic *N*-Mannich bases of azole were docked with COVID-19 main protease in complex with an inhibitor N3 (PDB id: 6lu7). Among 32 ligand molecules, around 25 ligands showed an excellent binding score when compared to the standard drug favipiravir. The presence of dimethyl group in the pyrazole nucleus helps good interaction with protease enzyme. Among the Mannich bases, the secondary amine mannich base of piperazine considered as the best derivative to inhibit the protease enzyme.

Keywords: COVID19, Azole antiviral, Mannich bases.

INTRODUCTION

COVID-19 becomes an outrageous disease throughout the world. The flare-up of this disease was spotted at Wuhan, the largest metropolitan area of China in December 2019. Around 20 years, before this coronavirus several epidemics were there includes 'severe acute respiratory syndrome coronavirus' SARS-CoV (2002-2003), 'Middle East respiratory syndrome coronavirus' MERS-CoV (2012) [1]. A symptom of the COVID 19 begins at the beginning of December 2019 [2] and at the first stage, it was identified as pneumonia of unknown etiology. The Chinese Center for Disease Control and Prevention (CDC) investigated and found that the new virus belonging to the coronavirus family Coronaviruses (CoVs) are the biggest gathering of infections having a place with the *Nidovirales* request, which incorporates *Coronaviridae*, *Arteriviridae* and *Roniviridae* families. The *Coronavirinae* contains one of two subfamilies in the *Coronaviridae* family, with the other being the *Torovirinae*. The *Coronavirinae* are additionally subdivided into four gatherings, the α-, β-, γ- and δ-coronaviruses [3]. The infections were at first arranged into these gatherings dependent on serology, which are currently partitioned by phylogenetic bunching.

Coronavirus virions are round with breadths of around 125 nm as delineated in ongoing examinations by cryo-electron tomography and cryo-electron microscopy. The most conspicuous element of coronaviruses is the club-shaped spike projections exuding from the outside of the virion. These spikes are a characterizing highlight of the virion and give them the presence of sun-powered crown, provoking the name, coronaviruses. Coronaviruses have helically even nucleocapsids, which is unprecedented among positive-sense RNA infections, however undeniably increasingly basic for negative-sense RNA infections. Coronavirus infection particles contain four principle auxiliary proteins. These are the spike (S), layer (M), envelope (E), and nucleocapsid (N) proteins, which are all encoded inside the 32 end of the viral genome.

The SERS-CoV genome encodes various proteins. The replica quality, which is a significant segment of the CoV genome encoded for 16 NSPs as two enormous PPs (PP1a and

PP1ab). Two sorts of cysteine proteases follow up on these PPs to discharge the NSPs. The C-terminal finish of these PPs is separated by chymotrypsin-like cysteine protease (principle protease [Mpro] or 3C-like protease [3CLpro]) and the N-terminal end is prepared by the Mpro (otherwise called papain-like protease [PLpro]). The initial three cleavage locales of the PPs are cut by PLpro while the rest 11 destinations are divided by CLpro, and this cleavage brings about the arrival of 16 NSPs.

In the RCSB database, only one (PDB ID: 6LU7) is there on the 2019-nCoV, which is in complex with N3 (inhibitor). The total succession of the 2019-nCoV is available. However, it is just 95% like bat-SL-CoVZC45 and 88% to SIRS CoV-ZSc (nucleotide impact, NCBI. This features the measure of recombination procedures or changes that happened in the 2019-nCoV and changes in protein auxiliary and practical levels [4]. In this study, a molecular modeling technique is utilized to find out the excellent moiety to inhibit the protease enzyme that is present in the coronavirus. From literature found that azoles [5,6] are having the ability to inhibit the protease enzyme [7,8]. So some azoles were considered [9-11], which can link with primary and secondary amines through the Mannich base [12,13] reaction process.

EXPERIMENTAL

Databases: For the docking purpose, 32 synthetic ligand of 4 different azole nucleus and an approved antiviral drug against viral protease was utilized. The desired ligands were drawn in ChemSketch software. The SMILES notation [Simplified Molecular Input Line Entry System, which is a file format] of the ligands were generated. Files were saved in PDB format. The ligands were opened in Autodock 4.2 [14-16] tools which automatically add the gasteiger charges, non-polar hydrogen and assigns Auto dock type to each atom. After finding the root and root expansion, the number of torsions was set and file was saved in pdbqt format for further processing.

Drug likeness properties: Lipinski's rule of five helps to find the drug likeness score by evaluating the oral absorption property of the ligand. Solubility, diffusion, log P, molecular weight etc are evaluated. Lipinski's rule of five [17,18] can be found out by using Molinspiration server [19,20].

Molecular docking: The Auto dock 4.2 suite [21,22] was used to carry out molecular docking simulations of the designed database. The protein COVID-19 main protease in complex with an inhibitor N3 (PDB id: 6lu7) was downloaded from protein data bank. The crystal structure of the target protein was refined by removing the ligand and the water molecules to minimize the energy by using accelrys discovery studio. After refining the protein the PDB format is opened in the auto dock 4.2 software. Auto Dock will automatically add Kollmann charge and merge hydrogens. It saves the object in PDBqt format. The grid-based approach was used to minimize the run time, the grid size was set to 60 × 60 × 60 xyz. Then the file was saved in gpf format to run the Auto grid. The auto grid programme was run in the command prompt and the file is save in glg format. For the auto dock running the protein and the ligands in the pdbqt format were opened and number of evaluations in genetic algorithm window. Default docking parameters were kept. During docking, the Lamarckian genetic algorithm was used to optimize the ligand conformation and 10 docking runs were performed for each ligand. The population size was set to 150, the number of generations was set to 27,000, and the maximum number of energy evaluations were set to 2,500,000 and save in dpf format. The auto dock programme was run in the command prompt and the file is save in dlg format. Results were analyzed [23] and snapshots were taken.

Azole *N*-Mannich bases: Azoles are five-membered ring compounds with two hetero atoms. Here, the azoles are linked with primary and secondary amine by Mannich base reaction. We have selected 4 azole moieties which includes 3,5-dimethyl pyrazole, indazole, benzimidazole and imidazole. These are linked by 8 different amines like *o*-phenylene diamine (OPD), aniline, *p*-aminobenzoic acid (PABA), *p*-amino sulphonic acid dibutylamine, piperazine, *N*-methyl piperazine and diphenyl amine.The structures of 32 azole *N*-Mannich bases used for molecular docking studies are shown in Fig. 1.

The active hydrogen present in the 1st nitrogen of dimethyl pyrazole undergo Mannich reaction with primary/secondary amine forms a methylene group linkage followed by amino group (**a1-a8**).

The active hydrogen present in the 1st nitrogen of indazole undergo Mannich reaction with primary/secondary amine forms a methylene group linkage followed by amino group compound (**a9-a16**).

The active hydrogen present in the 1st nitrogen of benzimidazole undergo Mannich reaction with primary/secondary amine forms a methylene group linkage followed by amino group (**a17-a24**).

The active hydrogen present in the 1st nitrogen of imidazole undergo mannich reaction with primary/secondary amine forms a methylene group linkage followed by amino group (**a25-a32**).

MM-GBSA: The binding free energy calculation helps to estimate binding affinities of small molecules with the target protein. In this study, Molecular Mechanics-combined with Generalized Born surface (MM-GBSA) method was used to evaluate binding free energies [23] of five ligand using Prime MM-GBSA approach. Energies of the ligand-receptor complexes were calculated using Prime MM-GBSA technology with all receptor residues being held frozen.

The binding free energy ΔG_{bind} was estimated using the following equation:

$$\begin{aligned}\Delta G_{bind} &= G_{complex} \_ G_{protein} \_ G_{ligand} \\ &= \Delta E_{MM} + \Delta G_{GB} + \Delta G_{SA} - T\Delta S \\ &= \Delta E_{vdw} + \Delta E_{ele} + \Delta G_{GB} + \Delta G_{SA} - T\Delta S\end{aligned}$$

where, ΔE_{MM} represent the gas-phase interaction energy between protein-ligand complex; ΔE_{vdw} is van der Waals energy contribution; ΔE_{ele} electrostatic energy contribution; ΔG_{GB} represents the polar; ΔG_{SA} represents the non-polar components of desolvation free energy and $T\Delta S$ is the entropy contribution at temperature T.

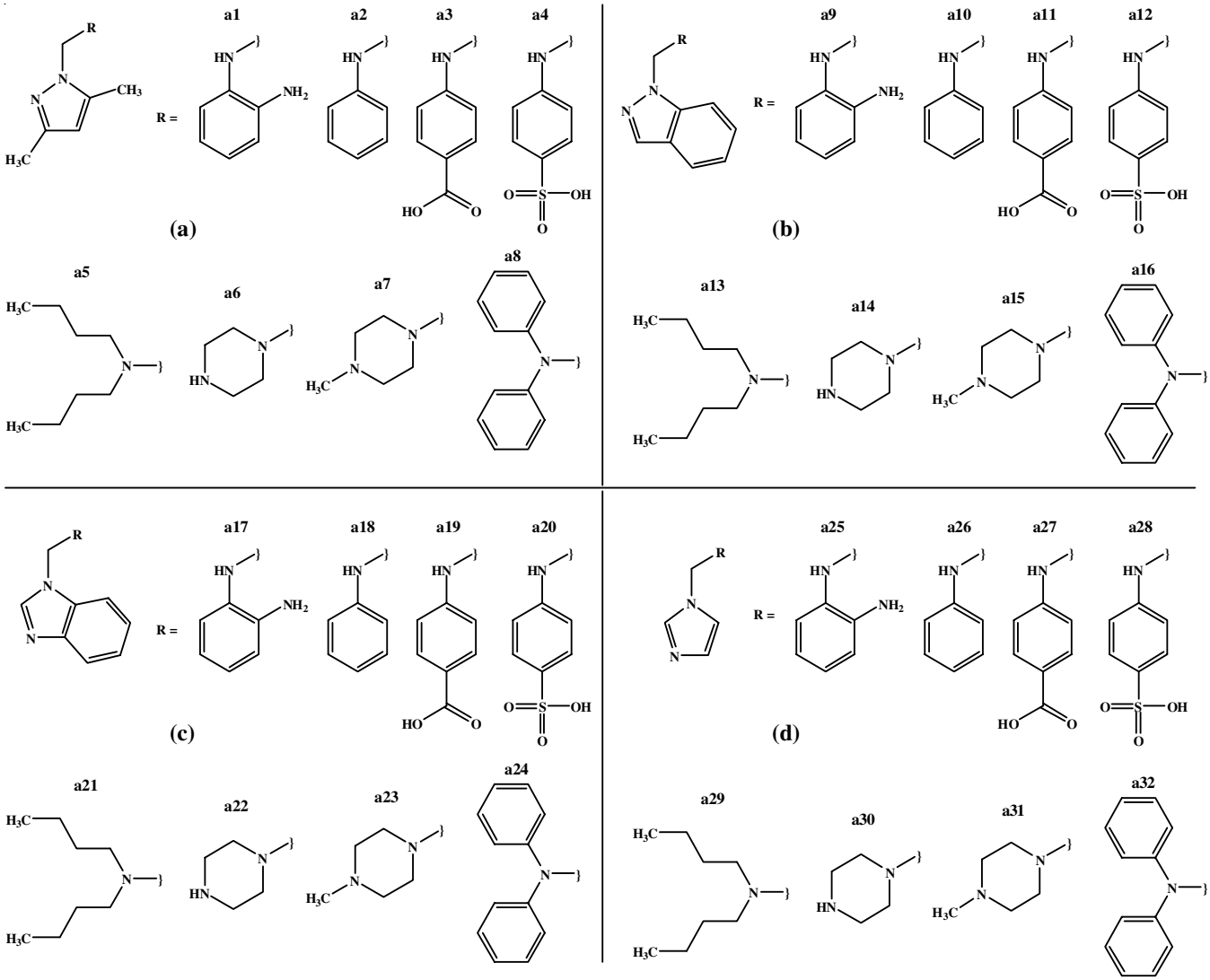

Fig. 1. Structures of (a) dimethyl pyrazole; (b) indazole; (c) benzimidazole and (d) imidazole and its derivatives

RESULTS AND DISCUSSION

Drug likeness property: In the present study, the *in-vivo* absorption capabilities of the designed molecules were assessed by the means of Lipinski's rule of five using molinspiration server. Lipinski's Rule of Five is a rule of thumb to evaluate drug likeness or determine if a chemical compound with a certain pharmacological or biological activity has properties that would make it a likely orally active drug in humans. Lipinski's rule says that, in general, an orally active drug should not have more than one violation such as Log P ≤ 5, molecular weight ≤ 500, the number of hydrogen bond acceptors ≤ 10, and the number of hydrogen bond donor's ≤ 5. All the 32 ligands satisfied the rule, indicating that the ligands **a1-a32** have good oral absorption (Table-1).

Molecular docking: Molecular docking is one of the widespread methods to explore the interactions between ligand and proteins. Docking reveals the efficient ligand molecule that has better binding with that of target and it also shows the H-bond binding affinity and π-π interactions. In this study, molecular docking was performed using autodock 4.2 software and novel azole *N*-Mannich base was docked against viral protease utilizing the structure of COVID-19 main protease in complex with an inhibitor N3. Autodock approach will computationally fit the ligand molecules in the 3D structure of the active site and ranking the ligands on the basis of interaction. All the studied ligand molecules of four different azole is linked with primary/secondary amine by Mannich base reaction were docked with the COVID-19 main protease in complex with an inhibitor N3 (PDB id: 6lu7). These ligands showed moderate to excellent activity against the standard drug favipiravir (Table-2, Fig. 2). The standard drug favipiravir showed a binding score of -4.59 Kcal/mol and the hydrophobic binding sites are TYR126, LYS-137, CYS128, GLN127, GLU290 and LYS5 with a inhibitory constant 428.85 μM. There are 3 hydrogen bond interactions with the amino acid residues (Fig. 3). The docking analysis of the 4 different azoles with *N*-Mannich bases of amines, some of the derivatives showed excellent binding interaction with viral protease. It has been ranked on the basis of lower the binding energy, stronger the binding affinity (Table-3).

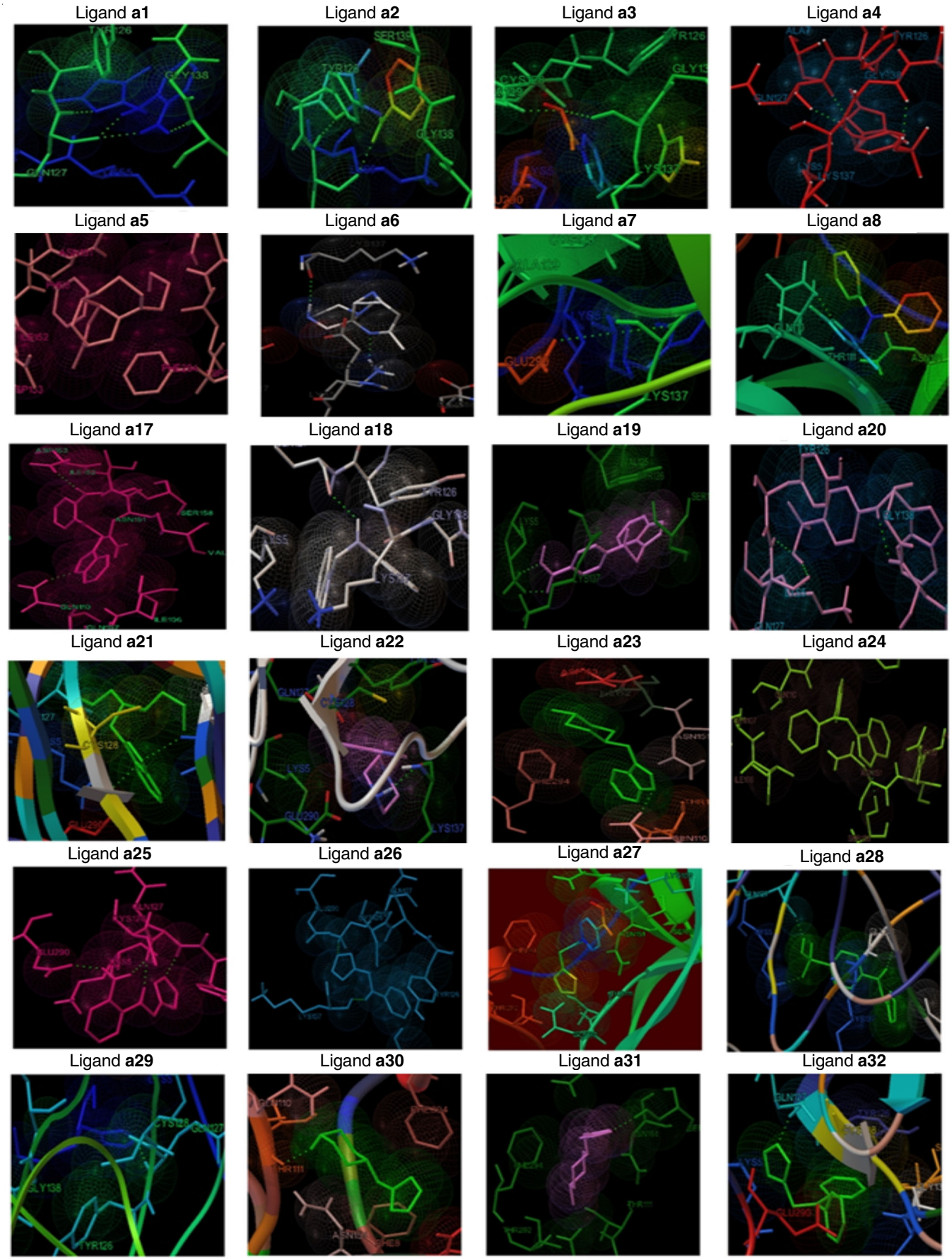

Fig. 2. 3D interaction plots of azole *N*-Mannich base ligands (a1-a32) against target protein COVID-19 main protease

TABLE-1
DRUG LIKENESS SCORES OF AZOLE *N*-MANNICH BASE LIGANDS (**a1-a32**) USING MOLINSPIRATION SERVER

Compound code	log P < 5	MW < 500	HBA < 10	HBD < 5	No. of violations
Pyrazole *N*-Mannich base					
a1	1.74	216.29	4	3	0
a2	2.30	201.27	3	1	0
a3	2.21	245.28	5	2	0
a4	-0.71	281.34	6	2	0
a5	3.72	237.39	3	0	0
a6	0.14	194.28	4	1	0
a7	0.74	208.31	4	0	0
a8	4.24	277.37	3	0	0
Indazole *N*-Mannich base					
a9	2.60	238.29	4	3	0
a10	3.16	223.28	3	1	0
a11	3.07	267.29	5	2	0
a12	0.15	303.34	6	2	0
a13	4.59	259.40	3	0	0
a14	1.01	216.29	4	1	0
a15	1.60	230.31	4	0	0
a16	5.11	299.38	3	0	1
Bezimidazole *N*-Mannich base					
a17	2.40	238.29	4	3	0
a18	2.97	223.28	3	1	0
a19	2.88	267.29	5	2	0
a20	-0.04	303.34	6	2	0
a21	4.39	259.40	3	0	0
a22	0.81	216.29	4	1	0
a23	1.41	230.31	4	0	0
a24	4.91	299.38	3	0	0
Imidazole *N*-Mannich base					
a25	0.90	188.23	4	3	0
a26	1.46	173.22	3	1	0
a27	1.38	217.23	5	2	0
a28	-1.54	253.28	6	2	0
a29	2.89	209.34	3	0	0
a30	-0.69	166.23	4	1	0
a31	-0.10	180.25	4	0	0
a32	3.41	249.32	3	0	0
Favipiravir (standard)	-0.52	157.10	5	3	0

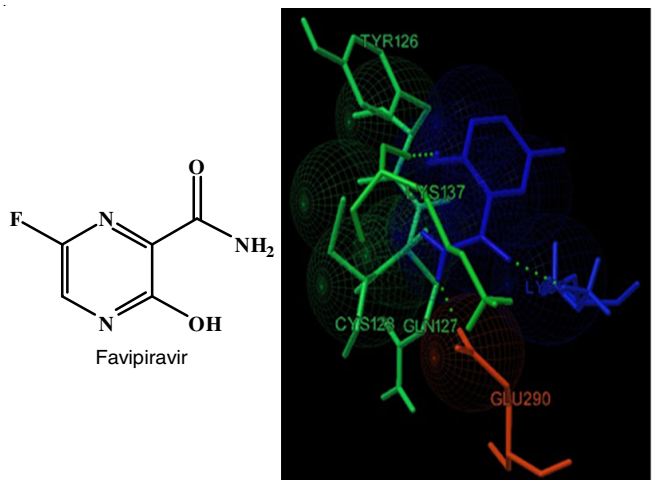

Fig. 3. Structure and 3D interaction plot of favipiravir against target protein COVID-19 main protease

TABLE-2
BINDING ENERGY OF AZOLE *N*-MANNICH BASE LIGANDS (**a1-a32**) AND STANDARD TOWARDS THE TARGET PROTEIN COVID-19 MAIN PROTEASE (PDB id: 6lu7)

Compound code	Binding energy (Kcal/mol)	No. of hydrogen bonding	Binding interaction (Hydrogen bonding)
Pyrazole *N*-Mannich base			
a1	-5.73	4	GLN127, GLY138,
a2	-5.01	2	GLN127, TYR126
a3	-4.72	2	ALA129, GLY138
a4	-4.65	3	GLY127, ALA7GLY138
a5	-5.13	0	No interaction
a6	-6.15	2	GLU290, LYS137
a7	-4.79	2	GLU290, GLY138
a8	-5.44	1	GLN110
Indazole *N*-Mannich base			
a9	-5.07	2	GLY170, GLU138
a10	-4.78	1	LYS5
a11	-4.62	2	LYS5, GLY138
a12	-4.98	3	LYS5, LYS137
a13	-3.95	1	GLN110
a14	-6.06	1	GLU240
a15	-5.72	2	LYS137, GLU290
a16	-4.78	1	GLN127
Bezimidazole *N*-Mannich base			
a17	-5.15	2	ASP153, GLN110
a18	-5.15	1	GLN127
a19	-4.72	2	LYS5
a20	-4.82	3	GLN127,TYR126,GLN138
a21	-3.49	2	LYS5, GLN127
a22	-5.38	1	LYS137
a23	-5.72	1	GLN110
a24	-5.58	1	SER158
Imidazole *N*-Mannich base			
a25	-4.44	4	GLU290, LYS5, TYR126
a26	-3.8	2	LYS5, LYS137
a27	-4.3	2	ASN151, GLN110
a28	-4.04	3	LYS5, GLN127, GLY138
a29	-3.2	1	CYS128
a30	-5.02	1	THR111
a31	-4.46	1	SASN151
a32	-5.34	1	GLN127
Favipiravir (standard)	-4.59	3	LYS5, LYS137, GLU290

Comparison of binding among pyrazole *N*-Mannich bases: From the docking results among 3,5-dimethyl pyrazole N-mannich derivatives (**a1-a8**) against the protein COVID-19 main protease, all the derivatives showed excellent binding energy against the standard drug. Among all the derivatives ligand, compound **a6** shown highest binding affinity of -6.15 Kcal/mol, 2 hydrogen bonding, an inhibitory constant of 30.93 μM and the binding interaction towards the residue GLU290, LYS137, GLN127, LYS5 and GLU288. Remaining 7 compounds also exhibit excellent binding interaction towards the enzyme. Binding of the ligands (**a1-a8**) are in the order: **a6** [piperazine *N*-Mannich base derivative] > **a1** [*o*-phenylene diamine *N*-Mannich base derivative] > **a8** [diphenylamine *N*-Mannich base derivative] > **a5** [dibutylamine *N*-Mannich base derivative] > **a2** [aniline *N*-Mannich base derivative] > **a7** [*N*-

TABLE-3
BINDING SCORES OF AZOLE *N*-MANNICH BASE LIGANDS (**a1-a32**) AGAINST DRUG FAVIPIRAVIR

Compound code	IUPAC name	Binding energy (Kcal/mol)
a1	*N*-[(3,5-Dimethyl-1*H*-pyrazol-1-yl)methyl]benzene-1,2-diamine	-5.73
a2	*N*-[(3,5-Dimethyl-1*H*-pyrazol-1-yl)methyl]aniline	-5.01
a3	4-{[(3,5-Dimethyl-1*H*-pyrazol-1 yl)methyl]amino}benzoic acid	-4.72
a4	4-{[(3,5-Dimethyl-1*H*-pyrazol-1-yl)methyl]amino}benzenesulfonic acid	-4.65
a5	*N*-Butyl-*N*-[(3,5-dimethyl-1*H*-pyrazol-1-yl)methyl]butan-1-amine	-5.13
a6	1-[(3,5-Dimethyl-1*H*-pyrazol-1-yl)methyl]piperazine	-6.15
a7	1-[(3,5-Dimethyl-1*H*-pyrazol-1-yl)methyl]-4-methylpiperazine	-4.79
a8	*N*-[(3,5-Dimethyl-1*H*-pyrazol-1-yl)methyl]-*N*-phenylaniline	-5.44
a9	*N*-(1*H*-Indazol-1-ylmethyl)benzene-1,2-diamine	-5.07
a10	*N*-(1*H*-Indazol-1-ylmethyl)aniline	-4.78
a11	4-[(1*H*-Indazol-1-ylmethyl)amino]benzoic acid	-4.62
a12	4-[(1*H*-Indazol-1-ylmethyl)amino] benzenesulfonic acid	-4.98
a13	*N*-Butyl-*N*-(1*H*-indazol-1-ylmethyl) butan-1-amine	-3.95
a14	1-(Piperazin-1-ylmethyl)-1*H*-indazole	-6.06
a15	1-[(4-Methylpiperazin-1-yl)methyl]-1*H*-indazole	-5.72
a16	*N*-(1*H*-Indazol-1-ylmethyl)-*N*-phenylaniline	-4.78
a17	*N*-(1*H*-Benzimidazol-1-ylmethyl)benzene-1,2-diamine	-5.15
a18	*N*-(1*H*-Benzimidazol-1-ylmethyl)aniline	-5.15
a19	4-[(1*H*-Benzimidazol-1-ylmethyl)amino]benzoic acid	-4.72
a20	4-[(1*H*-Benzimidazol-1 ylmethyl)amino]benzenesulfonic acid	-4.82
a21	*N*-(1*H*-Benzimidazol-1-ylmethyl)-*N*-butylbutan-1-amine	-3.49
a22	1-(Piperazin-1-ylmethyl)-1*H*-benzimidazole	-5.38
a23	1-[(4-Methylpiperazin-1-yl)methyl]-1*H*-benzimidazole	-5.72
a24	*N*-(1*H*-Benzimidazol-1-ylmethyl)-*N*-phenylaniline	-5.58
a25	*N*-(1*H*-Imidazol-1-ylmethyl)benzene-1,2-diamine	-4.44
a26	*N*-(1*H*-Imidazol-1-ylmethyl)aniline	-3.80
a27	4-[(1*H*-Imidazol-1-ylmethyl)amino]benzoic acid	-4.30
a28	4-[(1*H*-Imidazol-1-ylmethyl)amino]benzenesulfonic acid	-4.04
a29	*N*-Butyl-*N*-(1*H*-imidazol-1-ylmethyl)butan-1-amine	-3.20
a30	1-(1*H*-Imidazol-1-ylmethyl)piperazine	-5.02
a31	1-(1*H*-Imidazol-1-ylmethyl)-4-methylpiperazine	-4.46
a32	*N*-(1*H*-Imidazol-1-ylmethyl)-*N*-phenylaniline	-5.34
Favipiravir (standard)	6-Fluoro-3-hydroxypyrazine-2-carboxamide	-4.59

methyl piperazine *N*-Mannich base derivative] > **a3** [*p*-amino benzoic acid *N*-Mannich base derivative] > **a4** [*p*-amino sulphonic acid N-Mannich base derivative] > favipiravir)

Comparison of binding among indazole N-Mannich base: From the docking results among, N-Mannich bases of Indazole derivatives (**a9-a16**) were docked against the protein COVID-19 main protease. Among these compounds, all the compounds had shown excellent binding affinity except one derivative. The excellent binding affinity is shown by ligand **a14** [piperazine N-Mannich base derivative] of -6.06 Kcal/mol, one hydrogen bonding, an inhibitory constant of 35.91 μM and the binding interaction towards the residue GLU240, PRO108, PRO132 and GLN107. The least affinity is shown by **a13** [dibutylamine N-Mannich base derivative] of -3.95 Kcal/mol. Binding of the ligands (**a9-a16**) are in the order: **a14** [piperazine N-Mannich base derivative] > **a15** [*N*-methyl piperazine *N*-Mannich base derivative] > **a9** [*o*-phenylene diamine *N*-Mannich base derivative] > **a12** [*p*-amino sulphonic acid *N*-Mannich base derivative] > **a10** [aniline *N*-Mannich base derivative] > **a16** [diphenylamine *N*-Mannich base derivative] > **a11** [*p*-aminobenzoic acid *N*-Mannich base derivative] > favipiravir > **a13** [dibutylamine *N*-Mannich base derivative]).

Comparison of binding among benzimidazole *N*-Mannich base: From the docking results among *N*-Mannich bases of benzimidazole derivatives (**a17-a24**) were docked against the protein COVID-19 main protease. Among these compounds, all the compounds had shown excellent binding affinity except one derivative. The excellent binding energy is shown by ligand **a23** [*N*-methyl piperazine *N*-Mannich base derivative] of -5.72 Kcal/mol, 1 hydrogen bonding, an inhibitory constant of 64.68 μM and the binding interaction towards the residue ASP153, ILE 152, ASN151, THR111, GLN110 and PHE294.The least affinity is shown by **a21** [dibutylamine *N*-Mannich base derivative]. Binding of the ligands (**a17-a24**) are in the order: **a23** [*N*-methyl piperazine *N*-Mannich base derivative] > **a24** [diphenyl amine *N*-Mannich base derivative] > **a22** [piperazine *N*-Mannich base derivative] > **a17** [*o*-phenylene diamine *N*-Mannich base derivative] > **a18** [aniline *N*-Mannich base derivative] > **a20** [*p*-amino sulphonic acid *N*-Mannich base derivative] > **a19** [*p*-aminobenzoic acid *N*-Mannich base derivative] > favipiravir > **a21** [dibutylamine N-Mannich base derivative].

Comparison of binding among imidazole N-Mannich base: From the docking results, among *N*-Mannich bases of imidazole derivatives (**a25-a32**) were docked against the protein

COVID-19 main protease. Among these compounds, only two compounds **a32** and **a30** had shown excellent binding energy of -5.34 Kcal/mol, 1 hydrogen bonding, an inhibitory constant of 121.67 µM and the binding interaction towards the residue GLN127, TYR126, CYS128, LYS5, GLU290, GLY138, LYS37, SER139 and -5.02 Kcal/mol, 1 hydrogen bonding, an inhibitory constant of 210.8 µM and the binding interaction towards the residue GLN110, THR111, ASN151, PHE8, ASP153 and PHE294. Binding of the ligands (**a25-a32**) are in the order: **a32** [diphenylamine *N*-Mannich base derivative] > **a30** [piperazine *N*-Mannich base derivative] > favipiravir > **a31** [*N*-methyl piperazine *N*-Mannich base derivative]> **a25** [*o*-phenylene diamine *N*-Mannich base derivative] > **a27** [*p*-amino benzoic acid *N*-Mannich base derivative] > **a28** [*p*-amino sulphonic acid *N*-Mannich base derivative] > **a26** [aniline *N*-Mannich base derivative] > **a29** [dibutylamine *N*-Mannich base derivative].

MM-GBSA: Energy calculations were carried out of all five ligand and standard to determine their binding affinities using MMGBSA method. The calculated ΔG binding energy for **a6**, **a23**, **a14**, **a1** and **a15** is given in Table-4, which clearly indicated that the ligands having the good binding affinity than that of the standard drug favipiravir.

TABLE-4
BINDING ENERGY SCORES USING MMGBSA STUDY

Compound code	MMGBSA ΔG_{bind}
Favipiravir	-15.76
a6	-21.70
a23	-31.02
a14	-31.18
a1	-39.62
a15	-47.75

Conclusion

Among all the compounds, the pyrazole *N*-Mannich base derivative (Fig. 4) showed an excellent binding towards the target protein COVID-19 main protease. Comparing the *N*-Mannich base one can concluded that one of the necessities of protease inhibition is the attachment of alkyl groups or benzene ring showed excellent binding score towards enzyme protease as observed in dimethyl pyrazole, indazole and benzimidazole moiety. The presence of dimethyl group in the pyrazole nucleus helps in the good interaction of the protease enzyme. Among the Mannich bases, secondary amine Mannich base of piperazine (Fig. 5) considered as the best derivative to inhibit the protease enzyme. The long-chain secondary amine *i.e.* dibutylamine derivative showed the poor energy except in the pyrazole nucleus may because of the presence of a bulky group. It is concluded that dimethyl pyrazole *N*-piperazine derivative has a better drug candidate against covid-19. Subsequently, the drug likeness property satisfied the Lipinski′s rule of five and Ki is less that is needed for strong inhibitory effect. The drug-likeness model score revealed a positive score when compared with the standard drug. MMGBSA helps to find out the mnimum energy required for the binding of the lignads towards the COVID-19 protein.

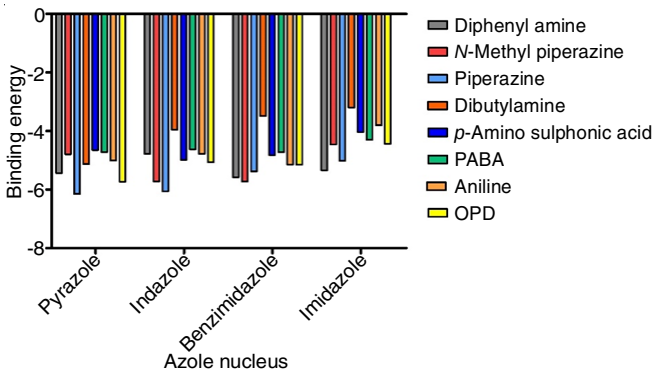

Fig. 4. Binding energy comparison of azoles among different *N*-Mannich bases

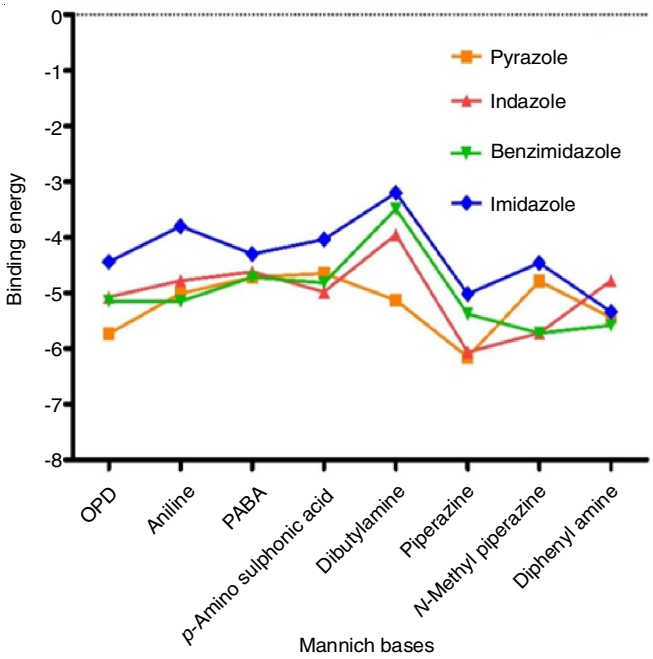

Fig. 5. Comparison of binding energy of derivatives of different azoles

CONFLICT OF INTEREST

The authors declare that there is no conflict of interests regarding the publication of this article.

REFERENCES

1. C. Marco, M. Rajnik, A. Cuomo, S.C. Dulebohn and R. Di Napoli, Features, Evaluation and Treatment of Coronavirus (COVID-19), In: StatPearls [Internet]. Treasure Island (FL): StatPearls Publishing (2021).
2. R.S. Joshi, S.S. Jagdale, S.B. Bansode, S.S. Shankar, M.B. Tellis, V.K. Pandya, A. Chugh, A.P. Giri and M.J. Kulkarni, *J. Biomol. Struct. Dyn.*, (2020); https://doi.org/10.1080/07391102.2020.1760137
3. A.R. Fehr and S. Perlman, *Methods Mol. Biol.*, **1282**, 1 (2015); https://doi.org/10.1007/978-1-4939-2438-7_1
4. T.J. Pallasc, *Periodontology*, **28**, 240 (2002); https://doi.org/10.1034/j.1600-0757.2002.280110.x
5. E. Rhoden, W.A. Nix, W.C. Weldon and R. Selvarangan, *Antiviral Res.*, **149**, 75 (2018); https://doi.org/10.1016/j.antiviral.2017.11.011
6. Z.Z. Hui, L.G. Lin, W. Hui and H.Z. Cheng, *Mini Rev. Med. Chem.*, **17**, 122 (2017); https://doi.org/10.2174/1389557516666160630120725

7. V.V. Zarubaev, E.L. Golod, P.M. Anfimov, A.A. Shtro, V.V. Saraev, A.S. Gavrilov, A.V. Logvinov and O.I. Kiselev, *Bioorg. Med. Chem.*, **18**, 839 (2010); https://doi.org/10.1016/j.bmc.2009.11.047
8. B. Medhi, M. Prajapat, P. Sarma, N. Shekhar, P. Avti, S. Sinha, H. Kaur, S. Kumar, A. Bhattacharyya, H. Kumar and S. Bansal, *Indian J. Pharmacol.*, **52**, 56 (2020); https://doi.org/10.4103/ijp.IJP_338_20
9. S. Vinoth Kumar, M.R. Subramanian and S.K. Chinnaiyan, *J. Young Pharm.*, **5**, 154 (2013); https://doi.org/10.1016/j.jyp.2013.11.004
10. K. Gullapelli, G. Brahmeshwari, M. Ravichander and U. Kusuma, *Egypt. J. Basic Appl. Sci*., **4**, 303 (2017); https://doi.org/10.1016/j.ejbas.2017.09.002
11. A. Ansari, A. Ali, M. Asif and S. Shamsuzzaman, *New J. Chem.*, **41**, 16 (2017); https://doi.org/10.1039/C6NJ03181A
12. J. March, Heterocyclic Chemistry, Textbook of Advanced Organic Chemistry, Reactions, Mechanisms and Structures, Wiley, pp 900-903 (1992).
13. R.K. Bansal, Heterocyclic Chemistry: Synthesis, Reactions and Mechanisms, New Age International (Pvt.) Limited, pp. 514-525 (1999).
14. S.M.D. Rizvi, S. Shakil and M. Haneef, *EXCLI J.*, **12**, 831 (2013).
15. S. Singh, B.K. Malik and D.K. Sharma, *Bioinformation*, **1**, 314 (2006); https://doi.org/10.6026/97320630001314
16. P.J. Eddershaw, A.P. Beresford and M.K. Bayliss, *Drug Discov. Today*, **5**, 409 (2000); https://doi.org/10.1016/S1359-6446(00)01540-3
17. G. Vistoli, A. Pedretti and B. Testa, *Drug Discov. Today*, **13**, 285 (2008); https://doi.org/10.1016/j.drudis.2007.11.007
18. D.E. Ammar and A.O. Anas, *J. Biomol. Struct. Dyn.*, (2020); https://doi.org/10.1080/07391102.2020.1758791
19. C.A. Lipinski, *J. Pharmacol. Toxicol. Methods*, **44**, 235 (2000); https://doi.org/10.1016/s1056-8719(00)00107-6
20. C.A. Lipinski, *Drug Discov. Today: Technol.*, **1**, 337 (2004); https://doi.org/10.1016/j.ddtec.2004.11.007
21. S. Forli, R. Huey, M.E. Pique, M. Sanner, D.S. Goodsell and A.J. Olson, *Nat. Protoc*., **11**, 905 (2016); https://doi.org/10.1038/nprot.2016.051
22. M.R. Nisha, D.V. Sakthivel and M.G. Michael, *J. Biomol. Struct. Dyn.*, (2020); https://doi.org/10.1080/07391102.2020.1752802
23. S. Genheden and U. Ryde, *Expert Opin. Drug Discov.*, **10**, 449 (2015); https://doi.org/10.1517/17460441.2015.1032936